Harnessing Symmetry Breaking in Soft Robotics: A Novel Approach for Underactuated Fingers

Ryman Hashem[1,2], Toby Howison[1], Agostino Stilli[2], Danail Stoyanov [2], Weiliang Xu[3], and Fumiya Iida[1]

Abstract— Soft robotics, an emerging domain in modern robotics, introduces innovative possibilities alongside challenges in controllability, particularly with multi-degree inflatable actuators. We present a novel manipulation method using underactuated soft fingers that addresses these challenges by harnessing symmetry breaking. Central to our approach is the mechanism of self-organization within a ring actuator equipped with five fingers. Typically considered a drawback, we exploit the actuator's buckling behavior to facilitate in-hand manipulation. This strategic utilization enables object motion in both clockwise and counterclockwise directions via system perturbations and adjustments in frequency and duty cycle parameters. Employing the self-organizing properties of our actuator, our method is empirically validated through simulations and real actuator experiments, demonstrating the system's ability in manipulating objects by leveraging the inherent flexibility and morphological advantages. The design enables two degrees of freedom with minimal input, allowing objects to rotate due to the actuator's self-organizing actions. This simplification of control mechanisms is essential for soft robotics manipulation. Our findings indicate that control systems in soft robotics can be significantly simplified, harnessing the adaptable behavior inherent in its morphology.

I. Introduction

In the realm of robotics, "in-hand manipulation" denotes the capability of a robotic hand or gripper to alter the orientation of objects through strategic contact points [1]. Roboticists explore dexterous robotic hands from two perspectives: anthropomorphic, which draws inspiration from the human hand's functionality and its well-documented 27 degrees of freedom (DoF), exemplified by innovations like the Shadow Dexterous Hand [2]; and technical solutions, which are specialized grippers designed to emulate a specific set of DoFs required for manipulating objects, such as advancements in soft gripper technology [3]. Bicchi et al. suggest that while anthropomorphic designs are appealing, the design of robotic hands should prioritise functionality, with soft robot grippers often outperforming anthropomorphic models by combining the strengths of both approaches [4], [5].

The Complexity of in-hand manipulation tasks is underscored by the challenge of replicating the sophisticated dexterity of the human hand with robotic actuators, a field in which research, particularly regarding soft dexterous

[1] Bio-Inspired Robotic Laboratory, Department of Engineering, University of Cambridge, UK.

[2] Wellcome / EPSRC Centre for Interventional and Surgical Sciences, University College London, UK. `r.hashem@ucl.ac.uk`

[3] Department of Mechanical and Mechatronics Engineering, University of Auckland, New Zealand.
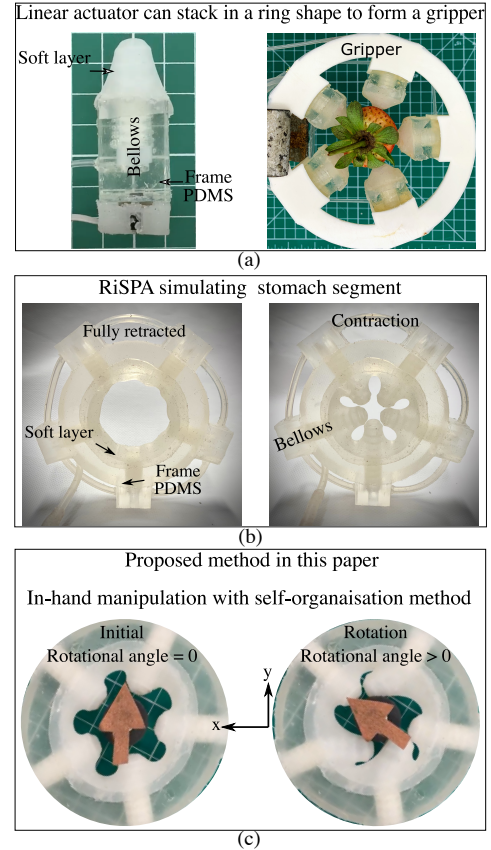
Fig. 1. The ring-shaped soft pneumatic actuator (RiSPA), featuring consistent morphology, has demonstrated versatility across various applications, including the manipulation of soft objects in (a), and the replication of human stomach or gastrointestinal tract segments in (b) as detailed in previous research [9], [10]. (c) highlights RiSPA's application in in-hand manipulation, where underactuated bellows (fingers) exhibit self-organising behavior to manipulate a cylindrical object, indicated by the arrow for visual guidance. The fingers naturally align in a single direction to facilitate rotation, showcasing self-organisation without external control. This adaptability across different tasks underscores the inherent morphological intelligence of the soft actuators.

actuators, remains sparse [6]. The precision required for controlling a dexterous hand with numerous DoFs presents another significant challenge, necessitating a manipulation approach that ensures trajectory adherence and uncertainty mitigation [7]. Here, the inherent compliance of soft materials, traditionally seen as a limitation, is redefined as a form of morphological intelligence that can be leveraged in control systems to reduce complexity, especially in underactuated systems [8].

Despite their basic designs, soft hand actuators leverage

the flexibility of soft materials to achieve complex manipulations with minimal control effort, a principle demonstrated in passive hand manipulation but underexplored in active soft prostheses [11], [12]. Soft actuators adeptly handle objects of various shapes and sizes, adjusting their orientation effortlessly without prior object knowledge, thereby outperforming rigid counterparts in terms of safety and adaptability during interaction with delicate items [13], [14], [15], [16].

Object manipulation with soft actuators employs the concept of moving contact points, a method encapsulated by the Equilibrium Point Manipulation (EPM) technique, which maintains slight, controlled contact alterations between the fingers and an object under manipulation forces [17]. This capability is crucial for telemanipulation scenarios, including surgical and humanoid robotics, as well as in prosthetic applications requiring object reorientation [18], [2].

Soft robotics has introduced many bio-inspired applications, benefiting significantly from the adaptive properties of their constituent materials. The concept of self-organisation, wherein a system naturally evolves into a stable state through dynamic interactions within its environment, plays a pivotal role in managing the abundant DoFs in soft robotic structures [19], [20]. This principle, often summarized as "order from noise," underpins the strategy of introducing perturbations to encourage soft robots to explore and adopt new stable configurations [21].

In biological systems, morphology and control mechanisms co-evolve to form entities capable of diverse functionalities [19]. Similarly, soft robots, designed to fulfill specific missions, exhibit the unique ability to adapt to multiple tasks with unchanged morphology. By integrating the dynamic interplay between morphology, control systems, and environmental interactions, soft robots can enhance their functionality, utilizing the multi-DoF morphology not as a challenge to be overcome but as an asset in control strategies.

Our prior research introduced a modular actuator capable of linear and gripping motions through a novel configuration (RiSPA), demonstrating its versatility across diverse applications with identical morphology, such as gripping functions and simulating biological contractions [9], [10]. Also, we briefly explored the manipulation mechanism while focusing on soft sensing during manipulation [22], [23]. This paper investigates the behaviour of soft bellows (fingers) during manipulation, highlighting its potential in in-hand manipulation to enhance robotic dexterity. Given that RiSPA is inherently underactuated system with self-organizing capabilities, we aim to address the challenges of control with a single input. We introduce a MATLAB simulations that resemble RiSPA under manipulation process. We illustrate how the unique morphology of soft actuators simplifies control strategies in underactuated systems by leveraging symmetry breaking.

II. MANIPULATION CONCEPT

We propose a ring actuator that manipulates objects with finger gating [1]. During actuation, the contact points between an object and a set of fingers alternate when the DoF
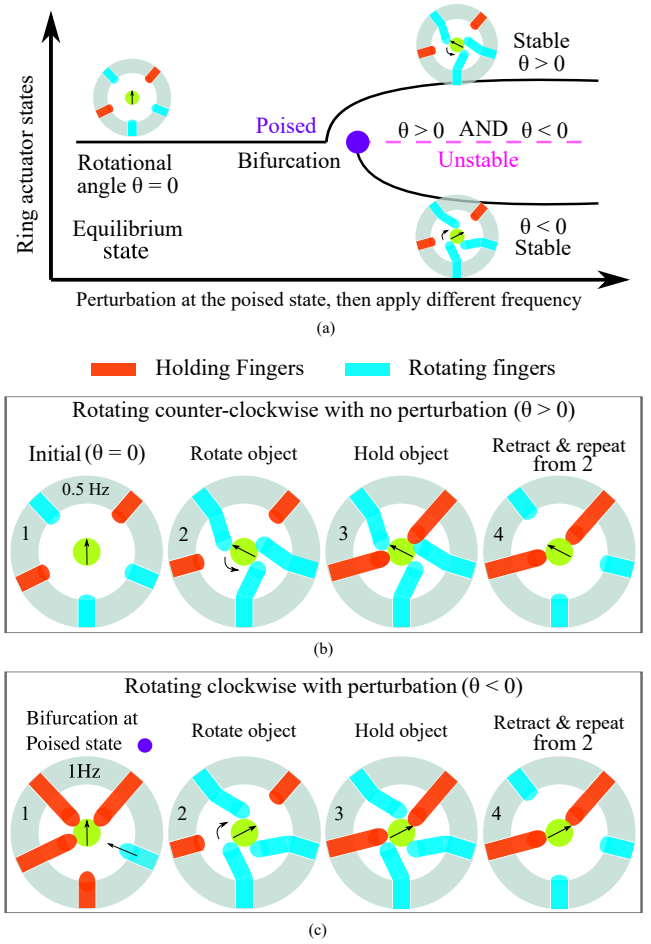

Fig. 2. The concept of the in-hand manipulation with soft ring actuator. (a) The illustration of the concept of bifurcation shift occurs on the ring actuator, where symmetry-breaking on the poised state dictates the rotation direction and stability as presented in a fork shape [24]. The system is considered stable when a rotation of one direction is maintained. The rotation direction is stimulated by external forces (altering frequency) that select a path on the fork when the system is poised. (b) The concept of breaking-symmetry is applied to the ring actuator (top view) to determine the rotation direction of the manipulated object: CW. (c) CCW rotation obtained by holding object with adjacent 3 fingers, retracting the fourth finger, while the fifth finger exert perturbation to the system that rotate objects ccw. From the poised state, the system is either stable or unstable, reaches an entropy path.

limit reaches. To envisage the actuation method with the proposed actuator, we can uncap a regular drink bottle with a twisting/rotational movement. There are multiple ways to unscrew the cap with a hand in a real-world scenario, usually by the thumb, pointer and middle. These three fingers are placed over the cap surface to form three contact points. Applying rotational forces to those points results in the unscrewing motion. As the rotational degree of the fingers is limited (related to the hand's joints anatomy, similarly in soft actuators), the process of unscrewing is repeated by alternating the contact points within the finger's range of motions without influencing the cap position. In contrast, the proposed ring actuator simulating this behaviour with some adjustments. RiSPA uses three fingers to rotate an object. While alternating the contact points to repeat the unscrewing motion, the other two fingers hold the object to stop the
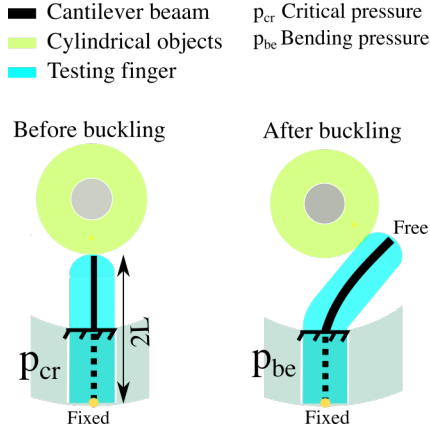
Fig. 3. A buckling test with cantilever beam to determine the applied pressure required for bending the finger. Three cylindrical objects were used with 22.5 mm, 20 mm, and 17.5 mm diameters. A single finger is used to analyse the critical and bending pressure depending on the finger's length.
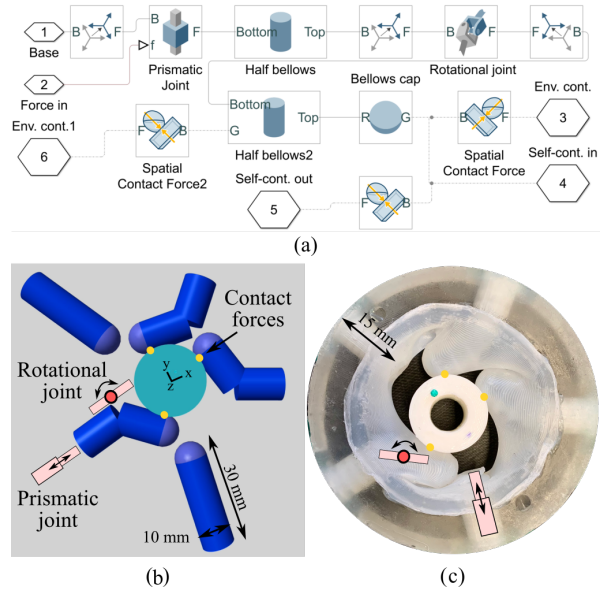

Fig. 4. The schematic illustration of the MatLab model of a single finger (a), the model of five fingers in (b), and RiSPA actuator in (c). The Simulink model consists of prismatic joint for transnational movements and rotational joint for the rotations on the X-Y plane. The interaction between fingers and objects is managed by adding spatial contact forces. The model finger parameters reflect RiSPA geometry.

rotational fingers from influencing the manipulation during both actuation and retraction.

The advantage of RiSPAs' fingers is the use of nonlinearity inherited in their material. By applying pressure to a finger, it will displace linearly. When a finger creates a contact point with than object and the displacement is restrained, the finger adjusts to the restrain by bending (buckling) left or right in the X-Y plane. This behaviour results in an underactuated system with a single input (applied pressure) and multiple outputs (prismatic and rotational joints). The direction (left or right) of the bending joint in the X-Y plane depends on many aspects, such as material properties, fabrication process, and initial conditions. Fig. 2 illustrates how symmetry is disrupted using RiSPA for in-hand manipulation. The concept is simplified by depicting the system's paths within an imperfect pitchfork bifurcation framework, reflecting the system's inherent symmetry and its predisposition towards a counterclockwise (CCW) direction. By introducing a perturbation, the manipulation is directed towards the alternative clockwise (CW) path, thereby breaking the symmetry. When fingers activate and touch an object, the system is stable and tends to rotate the object CCW (the primary path). Introducing a perturbation allows the system to adopt one of two states: rotating the object CW (the secondary path) or causing chaotic rotation (unstable). The point of bifurcation represents the moment of control over symmetry breaking, enabling the achievement of a specific directional rotation.

The self-organizing behavior of RiSPA is evident in the uniform direction of buckling exhibited by the five fingers. Regardless of whether all five fingers or only a subset are actuated simultaneously, they invariably buckle in the same direction, ensuring coherent movement without any conflicting actions among the fingers. This consistency guarantees the rotation of the object, either clockwise (CW) or counterclockwise (CCW). The underlying principle of this self-organization is attributed to the initial contact of a single finger with the object, which sets the direction for the subsequent buckling of the other fingers.

III. METHOD AND MODEL

A. Input Signal

Considering pressure is the only input, we identify three essential parameters to understand its impact on the system: signal amplitude, frequency, and duty cycle. Specifically, the amplitude is directly linked to the size of the object being manipulated. It determines how much the fingers move (displacement) and plays a role in whether the object buckles under pressure.

We used Euler's Column Formula and cantilever beam, as shown in Fig. 3 for calculating the bucking behaviour through the critical load applied to the soft finger:

$$load_{cr} = \frac{\pi^2 EI}{4\frac{1}{L^2}} \quad (1)$$

where E is the young modulus, I is the moment of inertia of the cross-section, and L is the finger's length when in contact with the object. The system is estimated as a cantilevered beam (free on one end and clamped on the other). The finger length is proportionally affect $load_{cr}$. The load is

TABLE I
SOFT FINGER CRITICAL AND BENDING APPLIED PRESSURE WITH THREE CYLINDRICAL OBJECTS.

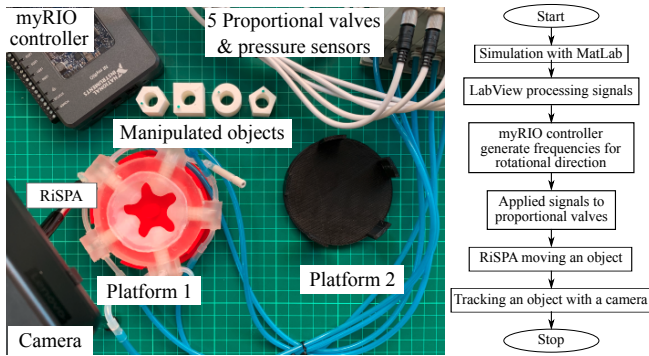| Parameters	17.5 mm	20 mm	22.5 mm
Model $p_c r$	72 kPa	66.3 kPa	58.9 kPa
Measured $p_c r$	70 kPa	60 kPa	50 kPa
Measured $p_b e$	90 kPa	70 kPa	70 kPa

Fig. 5. The experimental setup for tracking the rotation of the manipulated object on the platform and experimental platform architecture.

TABLE II
PARAMETERS FOR THE SOFT ACTUATOR MODEL.

Parameters	Values
Actuator mass	100.74 g [10]
Prismatic spring stiffness	28.126 N/mm [10]
Prismatic damping stiffness	8.225 N.s/mm [10]
Rotational spring stiffness	4.0e-04 N.mm/rad
Rotational damping stiffness	9.148e-05 N.s/mm
Static friction on contact forces	15
Dynamic friction on contact forces	0.5
Prismatic displacement boundaries	0-30 mm
Rotational displacement boundaries	0-55 $\theta°$
Fingers diameter	10 mm
Fingers Young's modulus	3 MPa
Fingers moment of inertia	531250 $g * mm^2$
Object mass	5 g

converted to pressure through $p_{cr} = load_{cr}/A_{eff}$, where $A_{eff} = \pi D_{mean}/4$. The model critical pressure and the real system are compared in Table I. The input errors stem from system fabrication issues and material behaviour, which are not fully captured by the redundant mathematical model.

The frequency and duty cycles significantly influence the behavior of manipulation as well. Within predefined boundaries, both frequency and duty cycles were examined to understand their impact on the system and to detect any instances of symmetry breaking. Consequently, a simulation system was created to explore object manipulation further and to resolve the equation of motion.

B. Simulation Model

The experimental approach alternates between RiSPA and a newly developed simulation in an iterative process. Initial experiments with RiSPA were conducted to determine the boundaries for applied pressure and frequency. The simulation facilitates exploration of potential object movements. As depicted in Fig. 4, the simulation includes a schematic and a model. The model features two joints: a prismatic joint, representing translational displacement, and a rotational joint, mimicking the bending of the actuator during buckling. This simplified model aids in analyzing the behavior of soft fingers. While increasing the DoFs could potentially enhance prediction accuracy, it also complicates parameter optimization. The interaction between the object and fingers is modeled using a spatial contact force block that employs a slip-stick friction model, incorporating both static and dynamic friction parameters. Nine parameters were required to be identified for the simulation models. Prior to this identification process, preliminary testing with the actual robot was crucial.

C. Experimental Setup

Fig. 5 displays the robot setup for conducting experiments. We utilised RiSPA from previous work [10]. A 3D model was designed to securely hold RiSPA in place, featuring either a centered post to limit the manipulated objects' DoFs, allowing only rotation along the z-axis (platform 1), or without a post, allowing the object to move freely on the x-y plane during the manipulation process (platform 2).

The incorporation of the post in platform 1 was essential for understanding the interaction between individual finger displacement and the objects' reactions during buckling. We employed cylindrical objects with diameters of 22.5 mm, 20 mm, and 17.5 mm as the manipulated objects (3D printed using PLA). The cylindrical shape was chosen to explore the proposed concept, while other objects and platform 2 are demonstrated in the supplementary material.

We used electro-pneumatic systems to control the ring, each finger connected to a proportional valve (ITV0030, SMC Japan). These valves are controlled by myRIO and LabView software (National Instrument), and includes pressure sensors that are monitored in LabView. A pulse function was used as applied signals with varied frequency and duty cycles. The amplitude was set from the buckling experiment (see Table I) for the rotating and holding fingers with different diameters. For example, manipulating a 22.5 mm object requires a minimum of 60kPa for rotating and a 50kPa for holding. The holding fingers have a phase delay of the half-time of the rotating fingers.

The tracking of the object's rotating angles on the Z-axes was measured by a video camera (Lenovo FHD Webcam) then the recordings were analysed by MATLAB to abstract the rotational angles of the objects. The objects were designed with notches that were coloured for detection.

D. Parameter Identification

The rotational behavior of the object was investigated using a configuration of three rotational fingers and two stabilizing fingers. A MATLAB script was created to fine-tune the parameters of the Simulink model, aiming to align with the initial outcomes observed with the ring actuator, specifically the object's rotational angles. The optimization process targeted nine parameters, as outlined in Table II, utilizing the Bayesian optimization method in MATLAB (bayesopt) across 1000 iterations. The optimization's objective function was the mean-squared error (immse) of the object's counterclockwise (CCW) rotation. The parameter boundaries were established based on the preliminary simu-
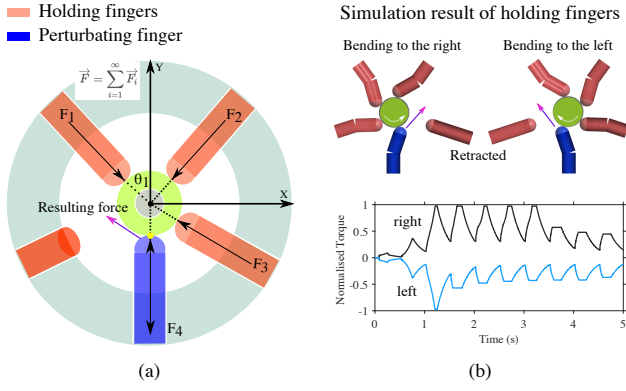
Fig. 6. Controlling the poised state through applied forces: (a) The resultant force vector acting on the object following the sum of forces $F_{1..4}$. Three fingers hold the object while one provides perturbation. A retracted finger directs the resultant force to rotate the object CW. (b) The simulation results of rotating the object CW and CCW, and the torque generated by the rotational joint of the holding finger.
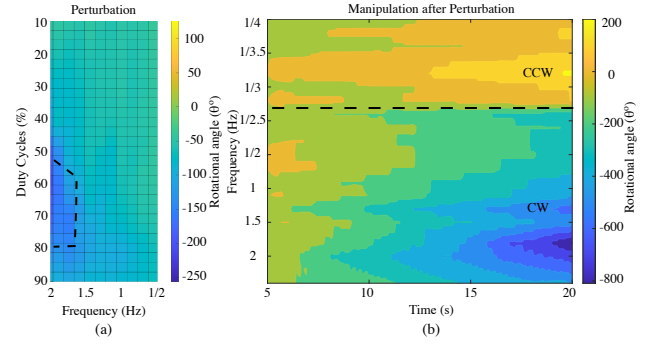

Fig. 7. (a) The effect of frequency and duty cycles on perturbation over 5 seconds. A frequency of 2 Hz and a 70% duty cycle are the optimal settings for rotating objects CW. (b) The impact of frequency on object manipulation following the perturbation process. A frequency of 1/2.6 Hz marks the threshold before the fingers bend in the preferred direction.

lation tests. The optimization included three rotational steps in the evaluation of the cost function.

E. Bifurcation Identification

Given the system has a preferable path (CCW), force analysis and simulation were utilized to pinpoint the bifurcation point and enable rotation in the clockwise (CW) direction. Fig. 6a displays the force vectors acting on the cylinder, where the direction of the resultant force determines the object's rotation. Here, three fingers stabilize the object, with one finger applying repeated force. The fifth finger, situated next to the force-applying finger, is fully withdrawn. The orientation of the withdrawn finger in relation to the force-applying finger influences the rotation direction: if the withdrawn finger is to the left, the object rotates CW, and vice versa, as illustrated in Fig. 6b.

The force-applying finger's effect was evaluated at various frequencies and duty cycles using a MATLAB sweep function and duration of 5 seconds. Frequencies of 0.5, 1, 2, and 3 Hz were tested. To avoid chaotic behavior, frequencies above 2 Hz are discouraged, while frequencies lower than 0.5 Hz are considered viable for slower actuations. The duty cycle of the signal was also varied from 10 to 90% in 10% increments, finding that a frequency of 2 Hz and a duty cycle of 70% produced the most effective perturbation. Fig. 7a illustrates how the perturbing finger's frequency and duty cycle influence the object's rotation.

Following a 5-second perturbation cycle that induces CW rotation, another series of tests assessed the frequency's impact on bifurcation. Fig. 7b presents simulation outcomes for the bifurcation analysis. Post-perturbation, achieving CW rotation is possible within the 1.5 to 2 Hz frequency range; below this threshold, the system tends to revert to the preferred CCW rotation path.

IV. RESULTS AND DISCUSSION

Fig. 8 (left) presents the comparison between simulated and actual rotational angles of the object at a 1 Hz frequency

without any perturbation. The actuator's performance closely matches the simulation, with a slight deviation of about 5% observed during a full rotation. Achieving 12 consecutive rotations within 25 seconds, the results indicate that, in the absence of perturbation, the object constantly rotates in a CCW direction, aligning with one of the desired stable states where $\theta > 0$. A staircase pattern was observed in the signal, with a slight drop after each rotation, attributed to the holding fingers preventing reverse rotation while the rotating fingers retract. Adjusting the phase delay and pressure of the holding fingers could enhance rotational efficiency.

Fig. 8 (right) details the CW results post a single perturbation at the poised state. The object slightly rotated during the perturbation, affecting the condition of the other holding fingers causing them to bend left and rotate the object in the CW direction. The CW rotation speed proved to be faster than CCW, with a full rotation in about 7 seconds, attributing to the increased frequency of 2 Hz in CW as opposed to 1 Hz in CCW. The actuator showed a 20% deviation from the simulation in CW rotation after 1 revolution, a larger discrepancy compared to the CCW results. This deviation is attributed to several factors, including the object's friction with the platform, which requires parameter tuning in the simulation.

These findings underscore how a break in symmetry can facilitate a state change to $\theta < 0$, leveraging the soft actuator's DoFs and incorporating system morphology as an aspect of its intelligence rather than considering it a drawback. The adaptive bending of fingers in both CW and CCW directions emphasizes the potential of soft robotics in manipulation tasks.

A supplementary video illustrates the CW and CCW object rotation, highlighting the switch between rotating and holding fingers, and demonstrates the simulation's fidelity in mimicking soft actuator dynamics. The video compares the simulation outcomes with actual soft actuator performance for both rotation directions. It also shows the manipulation of objects with different shapes on platforms 1 and 2, as shown in Fig. 5. Thus, it will demonstrate the capability of the proposed method regarding the break of symmetry,
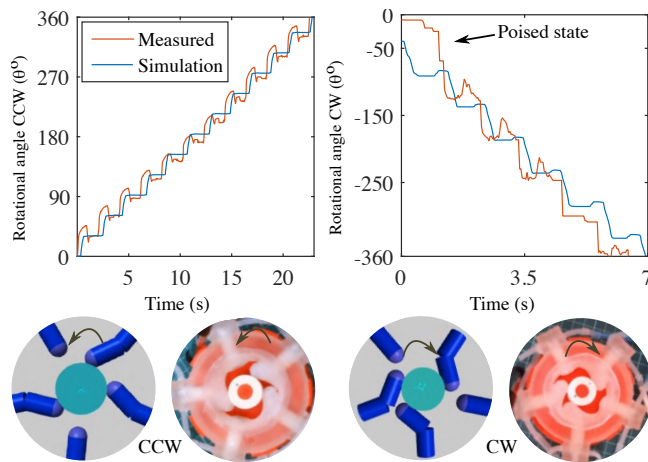
Fig. 8. Rotation outcomes depicting 360°revolutions: CCW at 1Hz and CW at 2Hz. The initial CW manipulation commences with a perturbation.

self-organization behavior, and underactuated manipulation. It has been observed that the shape of the object significantly impacts the repeatability of its manipulation. For instance, a cylindrical object can be manipulated with an accuracy of 90%, whereas a square object only achieves an accuracy of 40%. This discrepancy is attributed to the configuration of the 5 fingers arranged in a circle and how the 5 sides of the pentagon align perpendicularly with the fingers.In future work, we will incorporate a closed-loop system to manipulate complex objects by altering the control of the 5 fingers, coupled with object shape.

V. Conclusion

This study showcased how the morphological features of soft actuators facilitate the simplification of control strategies in underactuated systems. By manipulating the frequencies and duty cycles of applied pressure, the symmetry within the manipulation process was altered, enabling the control of object rotation in both clockwise and counter-clockwise directions using a single input. The experiment utilized a cylindrical object to illustrate this concept, employing simple control methods. The adaptability and elasticity of soft fingers were represented through prismatic and rotational joints within the simulation to mimic soft finger behavior accurately. In counter-clockwise rotations, the simulation closely matched the actual actuator performance with a minor 5% deviation, while a larger 20% discrepancy was observed in clockwise rotations, indicating the need for further refinements in the simulation, such as the inclusion of dynamic friction models.

References

[1] I. M. Bullock, R. R. Ma, and A. M. Dollar, "A hand-centric classification of human and robot dexterous manipulation," *IEEE transactions on Haptics*, vol. 6, no. 2, pp. 129–144, 2012.

[2] S. Li, X. Ma, H. Liang, M. Görner, P. Ruppel, B. Fang, F. Sun, and J. Zhang, "Vision-based teleoperation of shadow dexterous hand using end-to-end deep neural network," in *2019 International Conference on Robotics and Automation (ICRA)*. IEEE, 2019, pp. 416–422.

[3] L. Gerez, C.-M. Chang, and M. Liarokapis, "Employing pneumatic, telescopic actuators for the development of soft and hybrid robotic grippers," *Frontiers in Robotics and AI*, vol. 7, p. 169, 2020.

[4] A. Bicchi, "Hands for dexterous manipulation and robust grasping: A difficult road toward simplicity," *IEEE Transactions on robotics and automation*, vol. 16, no. 6, pp. 652–662, 2000.

[5] A. Bicchi and A. Marigo, "Dexterous grippers: Putting nonholonomy to work for fine manipulation," *The International Journal of Robotics Research*, vol. 21, no. 5-6, pp. 427–442, 2002.

[6] A. Dwivedi, Y. Kwon, A. J. McDaid, and M. Liarokapis, "A learning scheme for emg based decoding of dexterous, in-hand manipulation motions," *IEEE Transactions on Neural Systems and Rehabilitation Engineering*, vol. 27, no. 10, pp. 2205–2215, 2019.

[7] B. Sundaralingam and T. Hermans, "Geometric in-hand regrasp planning: Alternating optimization of finger gaits and in-grasp manipulation," in *2018 IEEE International Conference on Robotics and Automation (ICRA)*. IEEE, 2018, pp. 231–238.

[8] M. A. Devi, G. Udupa, and P. Sreedharan, "A novel underactuated multi-fingered soft robotic hand for prosthetic application," *Robotics and Autonomous Systems*, vol. 100, pp. 267–277, 2018.

[9] R. Hashem, M. Stommel, L. Cheng, and W. Xu, "Design and characterization of a bellows-driven soft pneumatic actuator," *IEEE/ASME Transactions on Mechatronics*, 2020. DOI: 10.1109/TMECH.2020.3037643.

[10] R. Hashem, S. Kazimi, M. Stommel, L. K. Cheng, and W. Xu, "A biologically inspired ring-shaped soft pneumatic actuator for large deformation," *Soft Robotics*, 2021. Accepted.

[11] B. Maat, G. Smit, D. Plettenburg, and P. Breedveld, "Passive prosthetic hands and tools: A literature review," *Prosthetics and orthotics international*, vol. 42, no. 1, pp. 66–74, 2018.

[12] J. Hughes, P. Maiolino, and F. Iida, "An anthropomorphic soft skeleton hand exploiting conditional models for piano playing," *Science Robotics*, vol. 3, no. 25, 2018.

[13] S. Abondance, C. B. Teeple, and R. J. Wood, "A dexterous soft robotic hand for delicate in-hand manipulation," *IEEE Robotics and Automation Letters*, vol. 5, no. 4, pp. 5502–5509, 2020.

[14] L. U. Odhner, L. P. Jentoft, M. R. Claffee, N. Corson, Y. Tenzer, R. R. Ma, M. Buehler, R. Kohout, R. D. Howe, and A. M. Dollar, "A compliant, underactuated hand for robust manipulation," *The International Journal of Robotics Research*, vol. 33, no. 5, pp. 736–752, 2014.

[15] D. Rus and M. T. Tolley, "Design, fabrication and control of soft robots," *Nature*, vol. 521, no. 7553, pp. 467–475, 2015.

[16] N. R. Sinatra, C. B. Teeple, D. M. Vogt, K. K. Parker, D. F. Gruber, and R. J. Wood, "Ultragentle manipulation of delicate structures using a soft robotic gripper," *Science Robotics*, vol. 4, no. 33, 2019.

[17] Y. Kwon, A. Dwivedi, A. J. McDaid, and M. Liarokapis, "Electromyography-based decoding of dexterous, in-hand manipulation of objects: Comparing task execution in real world and virtual reality," *IEEE Access*, vol. 9, pp. 37 297–37 310, 2021.

[18] M. Liarokapis and A. M. Dollar, "Deriving dexterous, in-hand manipulation primitives for adaptive robot hands," in *2017 IEEE/RSJ International Conference on Intelligent Robots and Systems (IROS)*. IEEE, 2017, pp. 1951–1958.

[19] R. Pfeifer, M. Lungarella, and F. Iida, "Self-organization, embodiment, and biologically inspired robotics," *science*, vol. 318, no. 5853, pp. 1088–1093, 2007.

[20] W. R. Ashby, "Principles of the self-organizing system," in *Facets of systems science*. Springer, 1991, pp. 521–536.

[21] H. Von Foerster, "On self-organizing systems and their envitonments," *Self-organizing systems*, 1960.

[22] R. Hashem and F. Iida, "Embedded soft sensing in a soft ring actuator for aiding with the self-organisation of the in-hand rotational manipulation," in *2022 IEEE 5th International Conference on Soft Robotics (RoboSoft)*. IEEE, 2022, pp. 498–503.

[23] D. Hardman, R. Hashem, and F. Iida, "Composite stretchable sensors for the detection of asymmetric deformations in a soft manipulator," in *2023 IEEE International Conference on Soft Robotics (RoboSoft)*. IEEE, 2023, pp. 1–6.

[24] S. Huang, "Where to go: breaking the symmetry in cell motility," *PLoS biology*, vol. 14, no. 5, p. e1002463, 2016.